Life Sciences 223 (2019) 9–21

Contents lists available at ScienceDirect

Life Sciences

journal homepage: www.elsevier.com/locate/lifescie

Bone marrow-derived mesenchymal stem cells attenuate severe acute pancreatitis via regulation of microRNA-9 to inhibit necroptosis in rats

Guodong Song[a,1], Zhilong Ma[a,1], Dalu Liu[b,1], Daohai Qian[c], Jia Zhou[d], Hongbo Meng[a], Bo Zhou[a], Zhenshun Song[a,*]

[a] Department of General Surgery, Shanghai Tenth People's Hospital, Affiliated to Tongji University School of Medicine, Shanghai 200072, China
[b] Shanghai Clinical Medical College of Anhui Medical University, Hefei, Anhui 230032, China
[c] Department of Hepatobiliary Surgery, Yijishan Hospital, Wannan Medical College, Wuhu, Anhui 241001, China
[d] Tongren Hospital, Shanghai Jiao Tong University School of Medicine, Shanghai 200336, China

ARTICLE INFO

Keywords:
BMSCs
miR-9
SAP
Necroptosis
RIPK1

ABSTRACT

Aims: Severe acute pancreatitis (SAP) is an acute disease of the digestive system accompanied by pancreatic necrosis. We have found that bone marrow-derived mesenchymal stem cells (BMSCs) can attenuate SAP, but the underlying mechanism remains unclear. The present study was conducted to explore the possible mechanisms by which BMSCs alleviate SAP.

Main methods: BMSCs and BMSCs engineered to overexpress microRNA (miR)-9 (miR-9-BMSCs) were transplanted into rat models of SAP via the tail vein. Pancreatic acinar cells (PACs) were isolated from rat pancreatic tissues and induced by tumor necrosis factor-α (TNF-α) in vitro.

Key findings: miR-9-BMSCs significantly reduced the systemic inflammatory response, impeded the necroptosis signaling pathway and promoted regeneration of damaged pancreas in vivo. miR-9-BMSCs secreted miR-9, which targeted the gene encoding receptor interacting protein kinase 1 in PACs induced by TNF-α, to inhibit necroptosis and ameliorate SAP.

Significance: miR-9-BMSCs can reduce SAP-induced injury to pancreatic tissues and PACs by regulating miR-9 to suppress necroptosis.

1. Introduction

Acute pancreatitis (AP) is the most common pancreatic disease worldwide and is the leading gastroenterological reason for hospitalization [1]. AP may develop into severe AP (SAP) with a mortality rate as high as 25% in up to 20% of AP cases [2,3]. In the progression of SAP, multiple organ dysfunction syndrome and systemic inflammatory response syndrome account for the majority of systemic complications and mortality; furthermore it has been confirmed that self-digestion of pancreatic acinar cells (PACs) follows premature intracellular protease activation [4]. The injury to PACs plays an important role in the release of damage-associated molecular patterns (DAMPs) and pro-inflammatory cytokines, including interleukin-1β (IL-1β), IL-6 and tumor necrosis factor-α (TNF-α), which have multiple biological functions in the development of SAP [5]. Therefore, investigations should concentrate on how to block necrosis of PACs and release of DAMPs in order to provide new therapeutic options for SAP.

Recently, a new concept called necroptosis has been presented which is a pathway of programmed necrosis involving receptor interacting protein kinase 1 (RIPK1), RIPK3 and mixed lineage kinase domain-like protein (MLKL) [6,7]. Necroptosis has been confirmed to mediate myofiber death [8], intestinal inflammation [9], pancreatic carcinoma [10] and other conditions. In addition, MLKL deficiency has been shown to protect mice from cerulean-induced AP [11]. Hence, the suppression of necroptosis in SAP may be a key feature of therapeutic strategies in the future.

Mesenchymal stem cells (MSCs) have been utilized in various fields including scaffold transplants [12], materials engineering [13], and tissue repairs [14] and so on. Our own previous research have demonstrated that MSCs have the capacity to alleviate the systemic inflammatory response and promote angiogenesis in SAP [15–18]; however, the mechanisms by which MSCs exert these therapeutic effects

* Corresponding author at: Department of General Surgery, Shanghai Tenth People's Hospital, Tongji University School of Medicine, Yanchang Road 301, Shanghai 200072, China.
E-mail address: zs_song@hotmail.com (Z. Song).
[1] Guodong Song, Zhilong Ma and Dalu Liu contributed equally to this work.

https://doi.org/10.1016/j.lfs.2019.03.019
Received 17 December 2018; Received in revised form 1 March 2019; Accepted 8 March 2019
Available online 09 March 2019
0024-3205/

still remain unclear. MicroRNAs (miRs) are short non-coding RNAs of about 22 nucleotides that regulate gene silencing by guiding Argonaute proteins to target sites in the 3′-untranslated region (3′-UTR) of mRNAs [19]. Recently, a clinical study found that the level of serum miR-9 was increased in AP patients and thus miR-9 may serve as a diagnostic and prognostic biomarker for AP [20]. However, the role of miR-9 in the ameliorative effect of MSCs on AP is poorly understood. Increasing evidence has demonstrated that MSCs can regulate the expression of some miRNAs to cause unexpected therapeutic effects [21]. Therefore, we hypothesized that miR-9 may be regulated by BMSCs to reduce the inflammatory response and inhibit necroptosis of PACs in SAP. This study was conducted to clarify the possible mechanisms by which BMSCs efficiently attenuate SAP with the involvement of miR-9.

2. Materials and methods

2.1. Patients and ethical approval

Human donor blood was obtained from 33 men and women divided into three groups (n = 11 per group): (1) normal, (2) mild AP (MAP) and (3) SAP. Diagnoses were based on APACHE-II scores [22] in the Department of General Surgery, Shanghai Tenth People's Hospital (Shanghai, China). Human experimental protocols were approved by the Shanghai Tenth People's Hospital Ethics Committees. All work was conducted in accordance with the Declaration of Helsinki (1964).

2.2. Induction of experimental SAP

Healthy wild-type male Sprague-Dawley rats weighing 180–200 g were purchased from Shanghai SLAC Laboratory Animal Co., Ltd. (Shanghai, China). The experimental protocol was approved by the Institutional Animal Ethics Committee of Shanghai Tenth People's Hospital. The SAP model was induced by retrograde perfusion of 3% sodium taurocholate (NaT; Sigma-Aldrich, St Louis, MO, USA) as previously described [16].

2.3. Cell isolation, culture and treatment

BMSCs were isolated from 4-week-old Sprague-Dawley rats and cultured in DMEM-LG (Invitrogen, Grand Island, NY, USA) complete medium as previously described [16]. PACs were isolated from the rats by a collagenase digestion procedure as previously described [23]. The isolated PACs were seeded into DMEM/Ham F-12 medium (Invitrogen) containing 20% fetal bovine serum at 37 °C in a humidified atmosphere with 5% CO_2.

2.4. Experimental protocol

In vivo, 36 rats were randomly divided into six groups (n = 6 per group) as follows: (1) normal control (NC) group; (2) sham group: rats were anesthetized by intraperitoneal injection of 5% pentobarbital and subjected to opening and closing the skin; (3) SAP group: rats were induced by NaT as described above; (4) Phosphate Buffered Saline (PBS) group: rats were injected with PBS (2.5 ml/kg body weight) via the tail vein 12 h after NaT induction; (5) BMSC group: rats were intravenously injected via the tail vein with prepared BMSCs (The cells were detached with 0.25% trypsin and 1 mM ethylenediaminetetraacetic acid, 5×10^6 cells/kg body weight) 12 h after NaT induction; and (6) miR-9-BMSC group: rats were treated with intravenous injections of miR-9-BMSCs (miR-9 mimic was transfected into BMSCs to construct miR-9-BMSCs in vitro, the cells were detached like BMSC group, 5×10^6 cells/kg body weight) 12 h after NaT induction. All groups of animals were euthanatized 72 h after injections.

In vitro, the isolated PACs were plated in 6-well plates with 5×10^4 cells/well with DMEM/Ham F-12 medium, prepared PACs were cultured with or without TNF-α (50 ng/ml, 10 μl/well; Sigma-Aldrich) for 24 h. PACs induced by TNF-α were co-cultured with rat BMSCs (1×10^5 cells/well) or miR-9-BMSCs (1×10^5 cells/well) using transmembrane plates for 24 h.

2.5. Serum amylase and lipase assay

The rats were euthanized and serum was obtained from the blood 72 h after induction of SAP. The serum activities of amylase and lipase were measured using colorimetric assay kits (BioVision, Milpitas, CA, USA) according to the manufacturer's protocols.

2.6. Histologic examination of pancreatic tissues

After euthanization, fresh rat pancreases were excised and preserved in 4% paraformaldehyde. Tissues were embedded in paraffin and 5-μm sections were processed for hematoxylin and eosin (H&E) staining. Severity of pancreatic injury was determined by pathological scores to estimate the following three aspects of SAP: (1) edema, (2) infiltration and (3) acinar necrosis as previously described [18].

2.7. ELISA

The levels of cytokines in the serum (IL-1β, IL-6, TNF-α, IL-4 and IL-10) were measured using ELISA kits (R&D Systems, Minneapolis, MN, USA) following the manufacturer's instructions.

2.8. RNA isolation and quantitative real-time PCR

Total RNA was extracted from frozen animal pancreatic issues, animal serum, human serum and PAC-cultured supernatant from each group using Trizol reagent (Invitrogen, Carlsbad, California, USA) according to the manufacturer's directions. qRT-PCR assays were performed using a KAPA qPCR Kit (Kapa Biosystems, Boston, MA, USA). GAPDH and U6 served as the endogenous control. The primer sequences are listed in Table 1. Relative expression of the target genes was analyzed using the comparative $2^{-\Delta\Delta CT}$ method.

2.9. Western blot

Total protein was extracted from pancreatic tissues and cells using ice-cold RIPA lysis buffer (Invitrogen). Equal amounts of total protein from each sample were resolved on sodium dodecyl sulfate-polyacrylamide gel electrophoresis (SDS-PAGE) gels and transferred to nitrocellulose membranes or polyvinylidene fluoride membranes. The membranes were immersed in 5% non-fat milk for 1 h to block non-specific binding and then incubated overnight at 4 °C with primary antibodies purchased from CST (Danvers, MA, USA) as follows: RIPK1, RIPK3, MLKL, phosphorylated-MLKL (p-MLKL), pancreatic and duodenal homeobox 1 (PDX1), pancreatic specific transcription factor 1 (PTF1) and regenerating islet-derived protein 4 (Reg4). The next day, after washing with PBST three times, the membranes were incubated with the corresponding secondary antibodies GAPDH (CST) for 30 min at 37 °C. The protein bands were visualized using an Odyssey scanner (LI-COR Biosciences, USA). Protein concentrations were normalized to GAPDH as an endogenous control.

2.10. Immunohistochemistry

The prepared 5 μm pancreas sections were dewaxed, rehydrated and washed with PBS. The sections were infiltrated in citrate buffer and heated in a microwave for 10 min for antigen retrieval. Next, the sections were incubated with 3% hydrogen peroxide for 10 min to inhibit endogenous peroxidase activity. The sections were then incubated with the primary antibodies from Abcam (Cambridge, UK) against RIPK1 (1:50), RIPK3 (1:50) or p-MLKL (1:100) overnight at 4 °C. Subsequent procedures were similar to previous descriptions [18].

Table 1
Primer sequences for qRT-PCR.

Gene	Forward (5′–3′)	Reverse (5′–3′)
IL-1β	CATCCAGCTTCAAATCTCAC	ACCACTTGTTGGCTTATGTT
IL-6	TCTCTCCGCAAGAGACTTCC	TCTTGGTCCTTAGCCACTCC
TNF-α	TGATCCGAGATGTGGAACTG	GGCCATGGAACTGATGAGAG
IL-4	TGTAACGACAGCCCTCTGAG	GACCGCTGACACCTCTACAG
IL-10	GGACAACATACTGCTGACAG	CATTCATGGCCTTGTAGACAC
RIPK1	TCCTCGTTGACCGTGAC	GCCTCCCTCTGCTTGTT
RIPK3	CCAGCTCGTGCTCCTTGACT	TTGCGGTCCTTGTAGGTTTG
MLKL	TCTCCCAACATCCTGCGTAT	TCCCGAGTGGTGTAACCTGTA
PTF1	CTGAGAAAGCTCTCACAGGC	CTTCCAGTTCAGAGTTCTGCC
PDX1	GCAGGATTGTGCCGTAACCTC	GAATGTTCTCCTTGTGTGTGGC
Reg4	GTGAGGCTACTCCTTCTGCTG	GTAGACCCATCAATCCACTGC
GAPDH	CGCTAACATCAAATGGGGTG	TTGCTGACAATCTTGAGGGAG

Primers	miR-9 (5′–3′)	U6 (5′–3′)
Reverse transcription	GTCGTATCCAGTGCAGGGTCCGAGGTATTCGCACTGGATACGACTCATAC	ACGCTTCACGAATTTGCGTGTC
Forward	GGCTCTTTGGTTATCTAGCT	CTGCTTCGGCAGCACATATACT
Reverse	GTGCAGGGTCCGAGGT	ACGCTTCACGAATTTGCGTGTC

2.11. Construction of rat models of overexpression of miR-9

An miR-9 mimic (using the following primers: sense, 5′-UCUUUG GUUAUCUAGCUGUAUGA-3′ and antisense, 5′-AUACAGCUAGAUAAC CAAAGAUU-3′) was constructed in an adeno-associated virus-8 (AAV-8) vector (System Biosciences, CA, USA) as previously described [24], then transformed into *Escherichia coli* DH5α cells (ThermoFisher, MA, USA) and amplified together with the packaging plasmid (pAAV-RC) and the helper plasmid (pAAV-Helper). A Tiangen kit (Beijing, China) was used to extract the plasmid. Thereafter, the plasmid was transfected into AAV-293 cells, and the cells and cultured supernatants were collected 48–72 h later. Cell debris was removed using freeze-thaw and centrifugation (2000 rpm, 5 min), and the supernatant consisting of the adeno-associated virus solution was retained. Adeno-associated virus solution was injected into the pancreatic tissue of the rats by retrograde pancreaticobiliary injection like NaT induction of SAP.

2.12. Dual luciferase reporter assay

A wild-type 3′-UTR fragment and a mutant 3′-UTR fragment of RIPK1 were extended by PCR and inserted downstream from the luciferase gene in the psiCHECK-2 vector (Promega, Madison, WI, USA). For dual luciferase assays, 293T cells were plated in 6-well plates, then co-transfected with 100 nM of miR-9 mimic or negative control (miR-NC) and 100 ng of luciferase reporter vectors. Luciferase activity was detected using a luciferase reporter assay system (Promega) 24 h after incubation following the manufacturer's protocol.

2.13. Cell transfection and interference

miR-9 mimic and miR-NC were purchased from GenePharma (Shanghai China). These molecular products were transfected into PACs or BMSCs using HiPerFect Transfection Reagent (QIAGEN, Valencia, CA, USA) following the manufacturer's instructions. siRNAs targeting rat RIPK1 (si-RIPK1) were purchased from GenePharma. The siRNA sequence was transfected into PACs using HiPerFect Transfection Reagent (QIAGEN) following the manufacturer's protocol. Efficacy of knockdown was performed by Western blotting and qRT-PCR analysis 48 h after operation. The different siRNA sequence used for transfections is given in Table 2.

2.14. Flow cytometry

Cell necrosis of PACs was determined by flow cytometry assay. PACs subjected to different treatments were collected and washed twice with PBS. The cells were then incubated with 100 μl of binding buffer and 5 μl of FITC-Annexin V (20 mg/ml; BD Pharmingen, San Diego, CA, USA) at room temperature in the dark for 20 min, followed by the addition of 5 μl of propidium iodide (PI) at 50 μg/ml in the dark for 5 min and 400 μl of binding buffer. After staining, the percentage of necrotic cells among 10,000 cells was analyzed using a flow cytometer (BD Biosciences, San Jose, CA, USA). The Q1 region represents necrotic cells.

2.15. Cell Counting Kit-8 (CCK-8) assay

Cell viability was determined by CCK-8 assay. Cells from each group of PACs were seeded into a 96-well plate at 10^4 cells/well. After 12, 24, 36 and 48 h of growth, equal amounts of CCK-8 reagent (Dojndo, Kumamoto, Japan) were added to each well for 2 h at 37 °C and the absorbance was measured at 450 nm using a microplate reader (BioTek, Winooski, VT, USA).

2.16. Lactate dehydrogenase (LDH) assay

Cell viability could also be detected using LDH assay (Thermo Scientific, Waltham, MA). LDH release in the medium is because of the loss of plasma membrane integrity when cells are in necrosis [25]. Briefly, 100 μl of cultured supernatant from the different groups of cells were transferred to 96-well plates and incubated with 100 μl of LDH reaction solution in the dark at room temperature for 30 min. The absorbance was measured at 490 nm according to the manufacturer's directions.

2.17. Statistical analysis

All data are presented as means ± standard deviation (SD) from at least three independent experiments. Experimental results were analyzed using Student's *t*-tests and one-way analysis of variance. $p < 0.05$ was considered statistically significant.

3. Results

3.1. miR-9-BMSCs inhibited the systemic inflammatory response to SAP in vivo

SAP rats were intravenously administered BMSCs and miR-9-BMSCs after induction by NaT. The levels of serum amylase and lipase in the

Table 2
Primer sequences for siRNA.

Gene	Sense (5′–3′)	Antisense (5′–3′)
RIPK1 (#1)	GGA ACA ACG GAG TAT ATA A	UUA UAU ACU CCG UUG UUC C
RIPK1 (#2)	GUC UUC GCU AAC ACC ACU A	UAG UGG UGU UAG CGA AGA C
RIPK1 (#3)	GGA TAA TCG TGG AGA TCA T	AUG AUC UCC ACG AUU AUC C

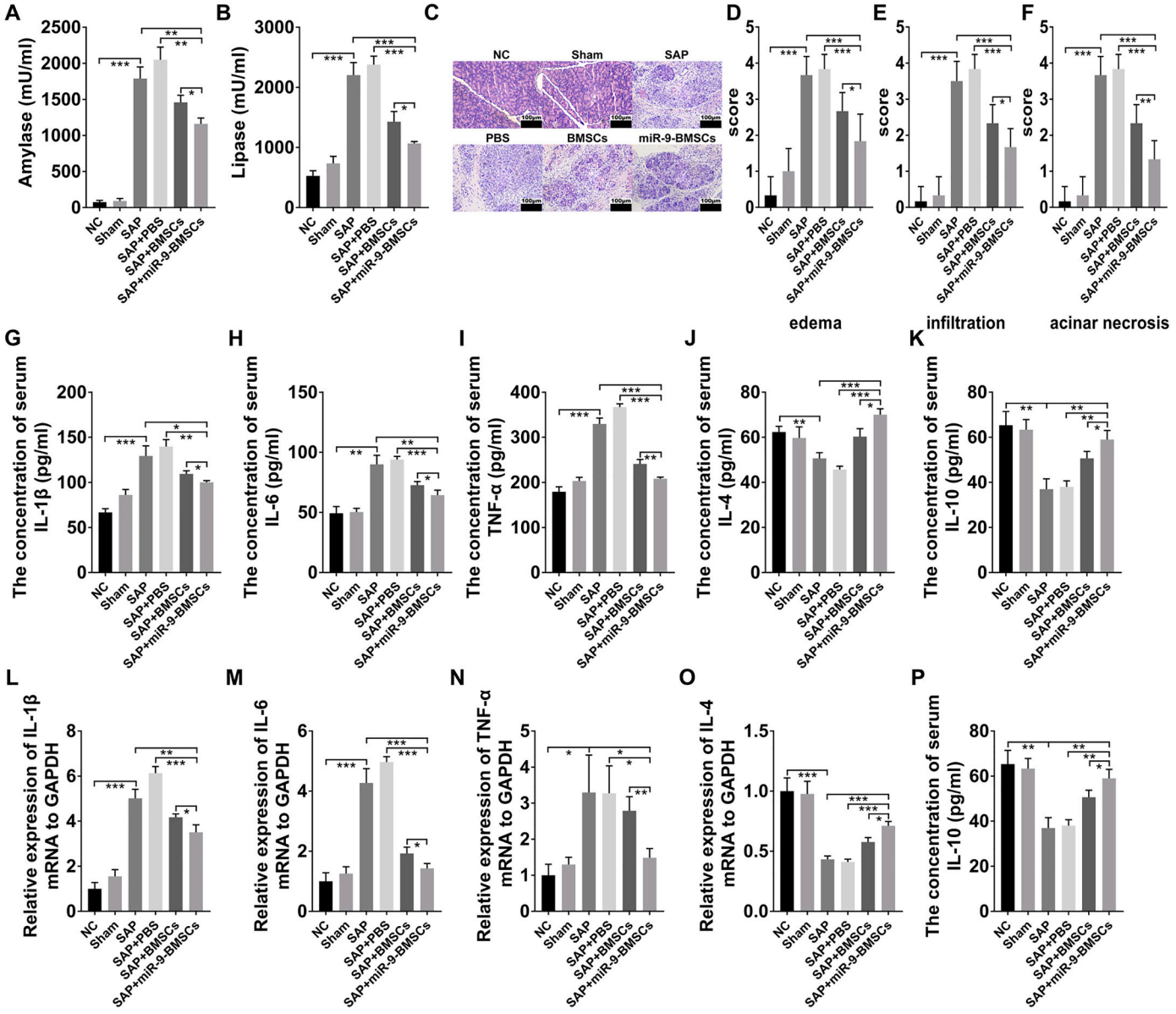

Fig. 1. miR-9-BMSCs alleviated NaT-induced SAP in vivo.
(A) Levels of serum amylase. (B) Levels of serum lipase. (C) H&E staining of pancreatic tissues. (D–F) Pathological scores for pancreatic edema, infiltration and acinar necrosis. (G–K) Levels of serum IL-1β, IL-6, TNF-α, IL-4 and IL-10 measured using ELISA. (L–P) Relative mRNA expression of pancreatic IL-1β, IL-6, TNF-α, IL-4 and IL-10 determined by qRT-PCR. Data are shown as means ± SD from at least three independent experiments. n = 6/group. Scale bar = 100 μm. $^{*}p < 0.05$, $^{**}p < 0.01$ and $^{***}p < 0.001$.

SAP group were much higher (Fig. 1A and B) than that in the NC group, as were the pathological scores for pancreatic edema, infiltration and acinar necrosis (Fig. 1C–F), and levels of pro-inflammatory cytokines IL-1β, IL-6 and TNF-α (Fig. 1G–I and L–N); however, the levels of anti-inflammatory mediators IL-4 and IL-10 showed the opposite results (Fig. 1J, K, O and P). In addition, transplanted miR-9-BMSCs markedly suppressed the levels of serum amylase and lipase (Fig. 1A and B), along with the extent of pancreatic edema, infiltration and acinar necrosis (Fig. 1C–F). Levels of pro-inflammatory cytokines (Fig. 1G–I, L–N) were reduced, and miR-9-BMSCs significantly enhanced the expression of anti-inflammatory mediators (Fig. 1J, K, O and P) compared with the SAP, PBS and BMSC groups.

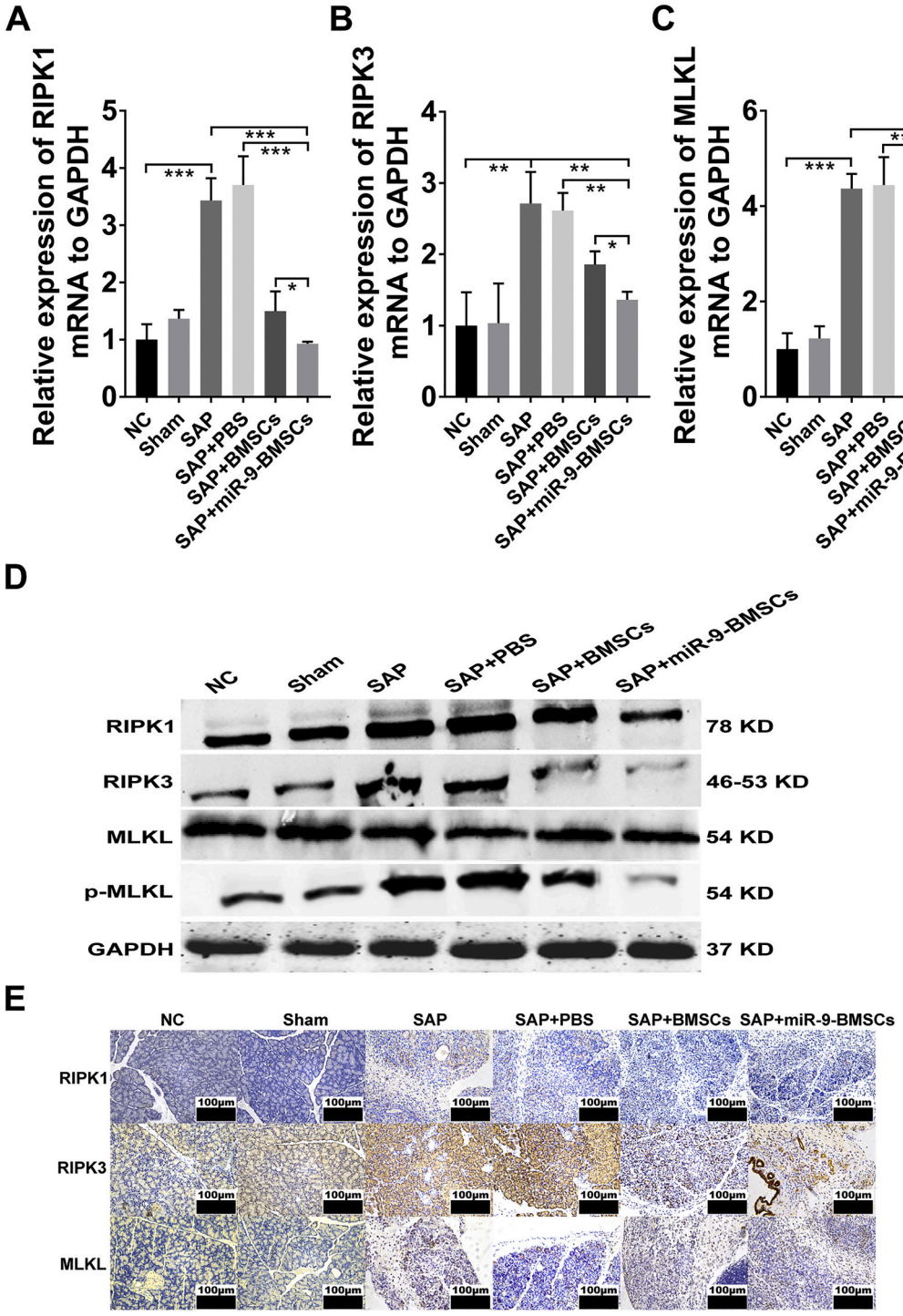

Fig. 2. miR-9-BMSCs suppressed necroptosis in SAP in vivo.
(A–C) Relative mRNA expression of pancreatic RIPK1, RIPK3 and MLKL detected by qRT-PCR. (D) Protein expression of pancreatic RIPK1, RIPK3, MLKL and p-MLKL determined by western blot. (E) Immunohistochemistry of pancreatic RIPK1, RIPK3 and p-MLKL. Data are shown as means ± SD from at least three independent experiments. n = 6/group. Scale bar = 100 μm. $^{*}p < 0.05$, $^{**}p < 0.01$ and $^{***}p < 0.001$.

3.2. miR-9-BMSCs suppressed the overexpression of necroptosis related proteins in the pancreas injured by SAP in vivo

In order to evaluate how miR-9-BMSCs alleviated SAP, we assessed the effect of miR-9-BMSCs on necroptosis signaling pathways by examining the expression of pancreatic RIPK1, RIPK3, MLKL and p-MLKL, which are all involved in necroptosis signaling. The expression of pancreatic RIPK1, RIPK3 and p-MLKL was much higher in the SAP group than that in the NC group, and was significantly inhibited by miR-9-BMSCs (Fig. 2A–D). Meanwhile, the downregulating effect of miR-9-BMSCs on necroptosis was clearly stronger than the effect of BMSCs (Fig. 2A–D). The immunohistochemistry results also supported this finding (Fig. 2E).

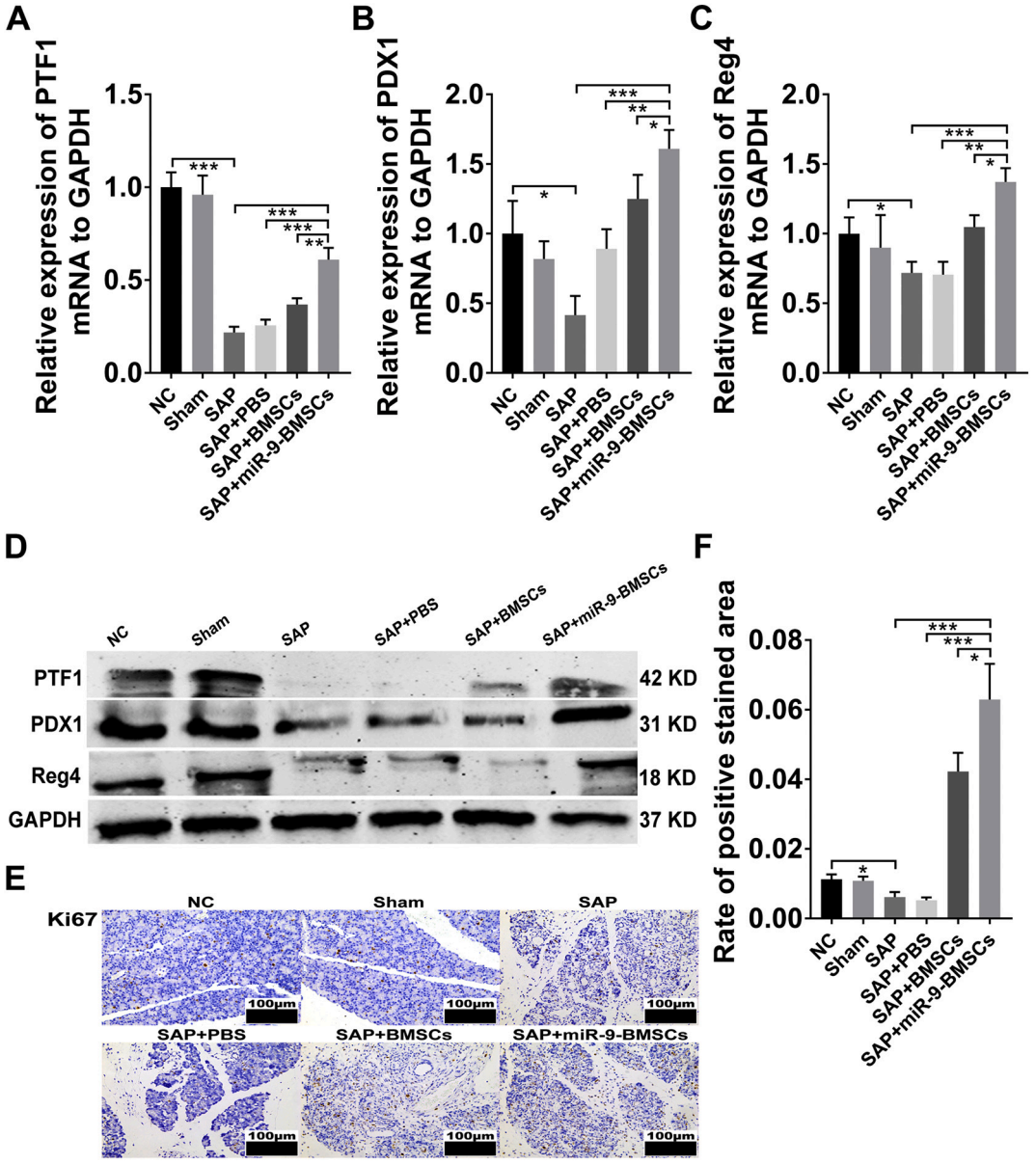

Fig. 3. miR-9-BMSCs promoted the regeneration of damaged pancreatic tissues in vivo.
(A–C) Evaluation of mRNA transcript levels of pancreatic PTF1, PDX1 and Reg4 determined by qRT-PCR. (D) Protein expression of pancreatic PTF1, PDX1 and Reg4 measured by western blot. (E) Immunohistochemistry of pancreatic Ki67 staining. (F) Rate of Ki67 positive stained area. Data are shown as means ± SD from at least three separate experiments. n = 6/group. $^{*}p < 0.05$, $^{**}p < 0.01$ and $^{***}p < 0.001$.

3.3. miR-9-BMSCs improved the repair of injured pancreas

To further examine whether pancreatic regeneration benefited from administration of miR-9-BMSCs, we assessed the expression of regenerative genes including PDX1 [26], PTF1 [27], and Reg4 [25]. Compared with the BMSC, SAP and PBS groups, miR-9-BMSCs significantly increased the expression of pancreatic PTF1, PDX1 and Reg4 (Fig. 3A–D). To show the direct evidence of pancreas regeneration, we performed Ki67 staining, and the immunohistochemistry results indicated that miR-9-BMSCs significantly promoted pancreatic regeneration compared with the BMSC, SAP and PBS groups (Fig. 3E and F).

3.4. miR-9 was positively correlated with AP

To evaluate the role miR-9 in AP, we collected serum samples from healthy donors, MAP patients and SAP patients. The results showed that the expression of serum miR-9 was much higher in the SAP group than that in the normal and MAP groups (Fig. 4A). In rats induced by NaT, serum miR-9 expression was much higher in the miR-9-BMSC group compared with the BMSC group (Fig. 4B), and NaT induction significantly decreased the expression of pancreatic miR-9 compared with the NC group (Fig. 4C). In addition, the expression of pancreatic miR-9 in the miR-9-BMSC group was significantly greater compared with the BMSC and PBS groups (Fig. 4C). We then utilized an AAV-8 vector to upregulate the expression of pancreatic miR-9 before NaT induction (Fig. 4D). Compared with the control AAV-8 group, overexpression of miR-9 not only decreased the levels of serum amylase and lipase (Fig. 4E); reduced the scores for pancreatic edema, infiltration and acinar necrosis (Fig. 4F and G); and diminished expression of serum pro-inflammatory cytokines (Fig. 4H), but also significantly enhanced the levels of anti-inflammatory mediators (Fig. 4H). Furthermore, upregulation of miR-9 markedly inhibited the expressions of pancreatic RIPK1, RIPK3, and p-MLKL, which play important roles in the

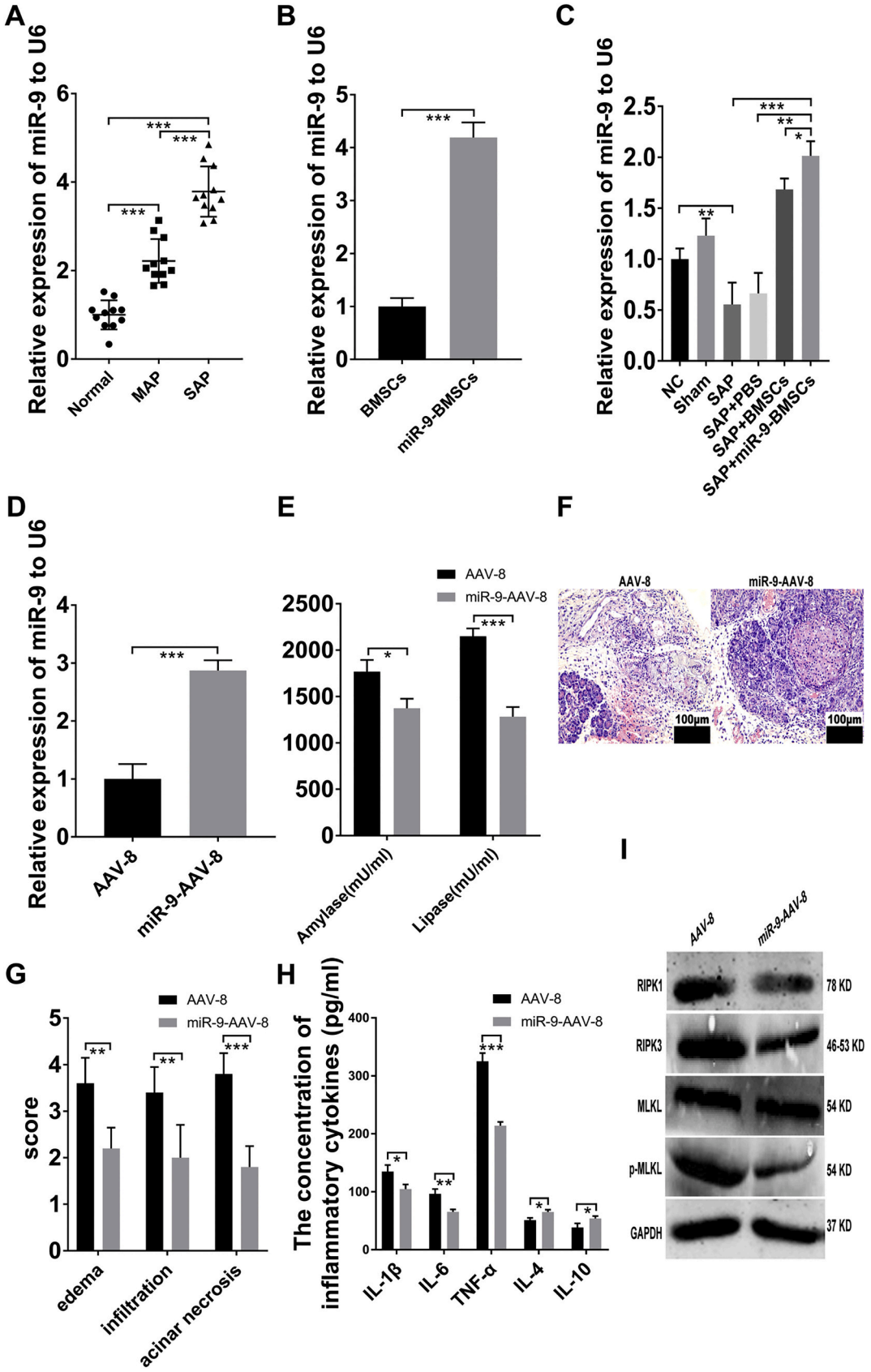

Fig. 4. miR-9 improved AP and SAP in vivo.

(A) Relative miR-9 expression in human serum detected by qRT-PCR. (B) Relative miR-9 expression in BMSCs and miR-9-BMSCs measured by qRT-PCR. (C, D) Relative miR-9 expression in pancreatic tissues from a rat model of AP determined by qRT-PCR. (E) Levels of serum amylase and lipase. (F) H&E staining of pancreas sections. (G) Pathological scores for pancreatic edema, infiltration and acinar necrosis. (H) Levels of serum IL-1β, IL-6, TNF-α, IL-4 and IL-10 measured using ELISA. (I) Western blot analysis of pancreatic RIPK1, RIPK3, MLKL, and p-MLKL. Data are shown as means ± SD for from least three independent experiments. n = 6/group. Scale bar = 100 μm. $^{*}p < 0.05$, $^{**}p < 0.01$ and $^{***}p < 0.001$.

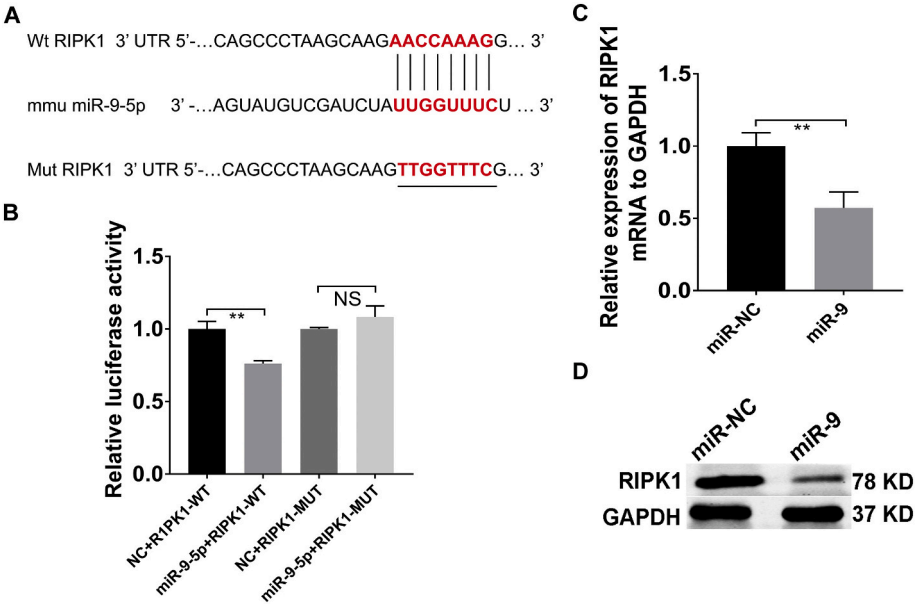

Fig. 5. RIPK1 was a direct target gene of miR-9.
(A) Structure of the 3′-UTR from wild-type RIPK1 (Wt-RIPK1) and mutant RIPK1 (mut-RIPK1) and paired bases between Wt-RIPK1 and miR-9. (B) Relative luciferase activities of Wt-RIPK1 3′-UTR and mut-RIPK1 3′-UTR after administration of miR-9 or miR-NC. (C) Relative expression of RIPK1 mRNA in PACs transfected with miR-9 mimic or miR-NC detected by qRT-PCR. (D) Protein expression of RIPK1 in PACs transfected with miR-9 mimic or miR-NC measured by western blot. Data are shown as means ± SD from at least three independent experiments. $^{**}p < 0.01$; NS, not significant.

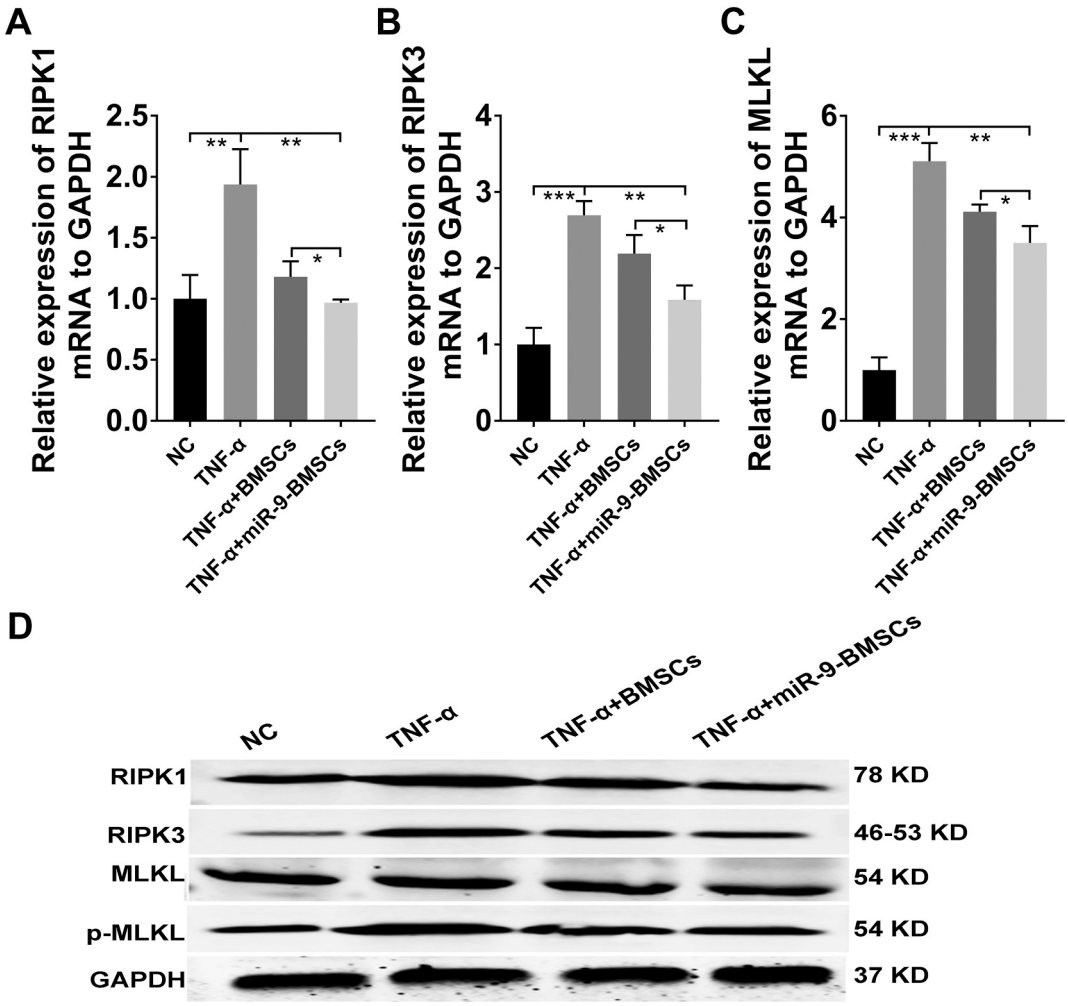

Fig. 6. miR-9-BMSCs inhibited necroptosis in TNF-α-induced-PACs in vitro.
(A–C) Assessment of mRNA expression levels of RIPK1, RIPK3 and MLKL in PACs after different treatments determined by qRT-PCR. (D) Protein expression of RIPK1, RIPK3, MLKL and p-MLKL in PACs from various groups measured by western blot. Data are shown as means ± SD from at least three independent experiments. $^{*}p < 0.05$, $^{**}p < 0.01$ and $^{***}p < 0.001$.

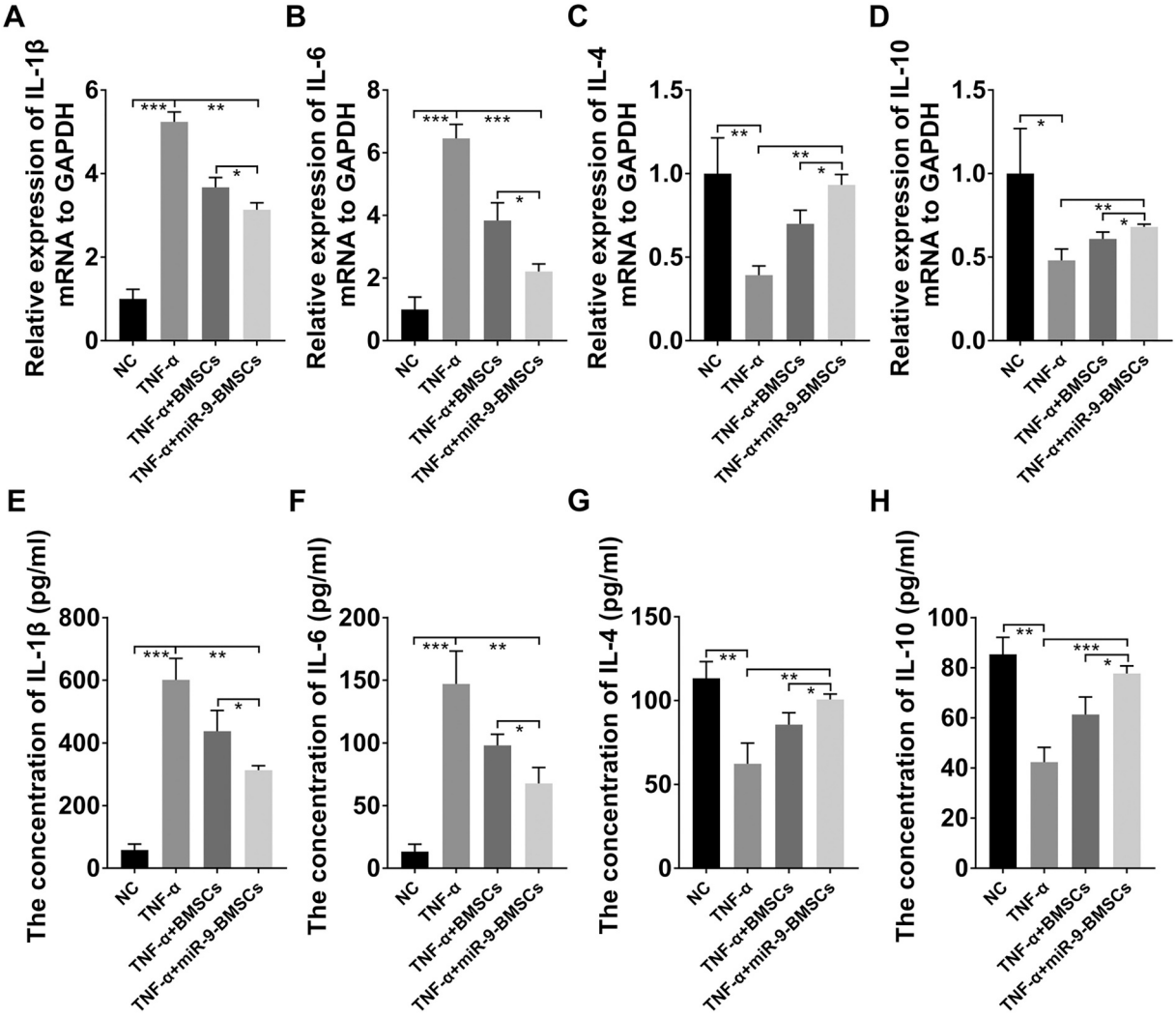

Fig. 7. miR-9-BMSCs decreased the inflammatory response of PACs treated with TNF-α in vitro.
(A–D) Relative mRNA expression of IL-1β, IL-6, IL-4 and IL-10 in culture supernatants detected by qRT-PCR. (E–H) Levels of IL-1β, IL-6, IL-4 and IL-10 in culture supernatants measured using ELISA. Data are shown as means ± SD from at least three independent experiments. $*p < 0.05$, $**p < 0.01$ and $***p < 0.001$.

necroptosis signaling pathway (Fig. 4I).

3.5. The target prediction and validation of miR-9

We used some miRNA target prediction programs such as TargetScan [28], miRWalk [29], and microRNA org [30] to seek the target genes of miR-9 and discovered that RIPK1 may be one such target. To determine if miR-9 could indeed directly target RIPK1, we performed dual luciferase reporter assays (Fig. 5A) and demonstrated that overexpression of miR-9 significantly decreased wild-type RIPK1 luciferase activity compared with the miR-NC group (Fig. 5B), while luciferase activity of the mutant RIPK1 3′-UTR construct remained unchanged (Fig. 5B). Furthermore, the expression of RIPK1 in the miR-9 group was much lower than that in the NC group (Fig. 5C and D).

3.6. miR-9-BMSCs inhibited the overactivation of the necroptosis signaling pathway in PACs induced by TNF-α in vitro

We isolated PACs from the pancreases of rats and seeded them into 6-well plates. To assess the effect of miR-9-BMSCs on necroptosis in vitro, we examined the expression of RIPK1, RIPK3, MLKL and p-MLKL. The results indicated that the expression of RIPK1 in cells treated with TNF-α was much higher than that in the NC group (Fig. 6A and D), as was expression of RIPK3 and p-MLKL (Fig. 6B–D). In addition, the suppressive effect on necroptosis in miR-9-BMSCs was much more intense than that in BMSCs (Fig. 6A–D).

3.7. miR-9-BMSCs reduced the inflammatory response of PACs treated with TNF-α in vitro

To further measure the levels of pro-inflammatory cytokines and anti-inflammatory mediators, we collected TNF-α-induced PACs and homologous supernatants. The findings showed that the expression of IL-1β and IL-6 increased significantly after induction by TNF-α (Fig. 7A, B, E and F), while the levels of IL-4 and IL-10 significantly decreased (Fig. 7C, D, G and H). After co-culture with BMSCs or miR-9-BMSCs, the levels of pro-inflammatory mediators and anti-inflammatory cytokines showed the opposite pattern of expression (Fig. 7A–H). In addition, compared with the BMSC group, miR-9-BMSCs inhibited the expression of more pro-inflammatory cytokines and increased the expression of more anti-inflammatory mediators (Fig. 7A–H).

3.8. miR-9-BMSCs and miR-9 promoted the viability of PACs treated with TNF-α in vitro

The viability of PACs after different treatments was analyzed by

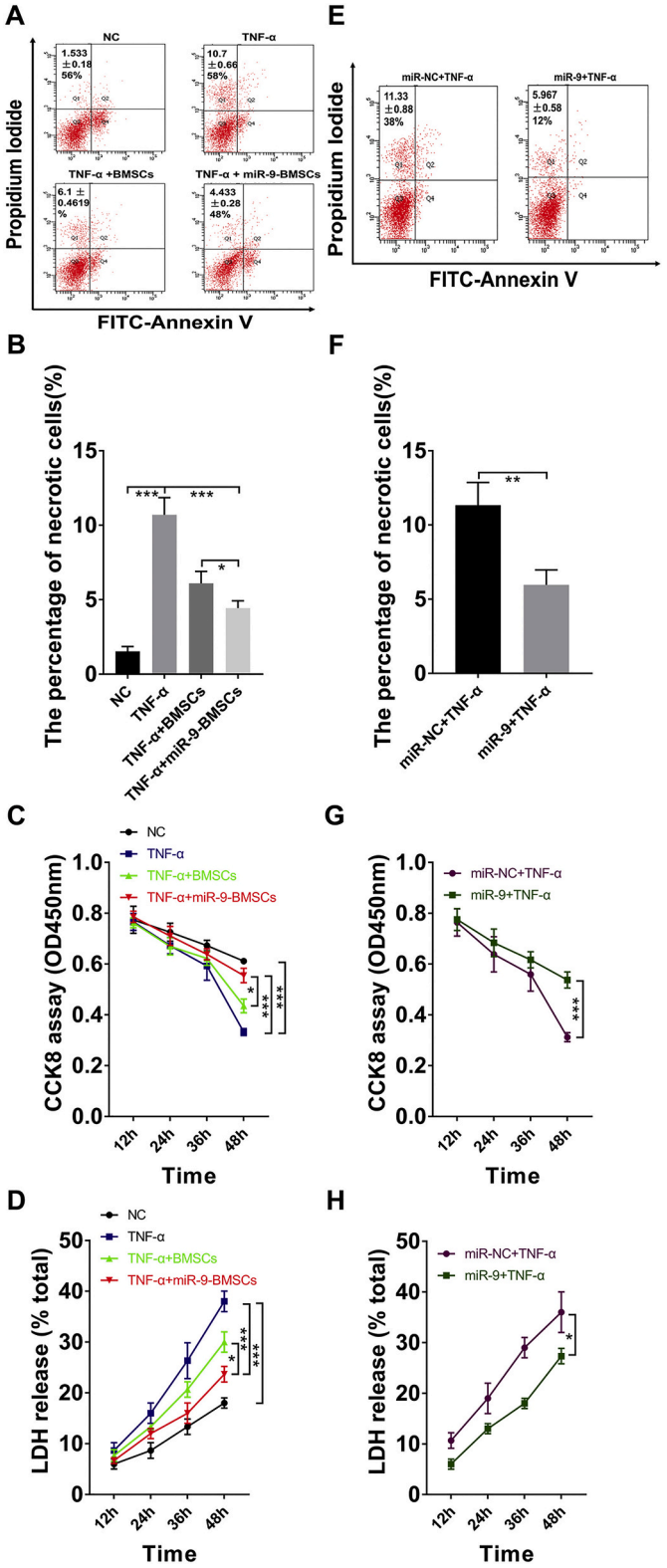

Fig. 8. miR-9-BMSCs and miR-9 improved the viability of PACs induced by TNF-α in vitro.

(A, E) PACs from various groups were collected and stained with FITC-Annexin V/PI and analyzed by flow cytometry. Figures are representative of three independent experiments. (B, F) Analysis of data from flow cytometry. (C, G) CCK-8 assays. (D, H) LDH release assays. Data are shown as means ± SD from at least three independent experiments. *$p < 0.05$, **$p < 0.01$ and ***$p < 0.001$.

flow cytometry, CCK-8 assays and LDH release assays. The results of these various assays suggested that administration of miR-9-BMSCs and transfection of miR-9 mimic both markedly suppressed necrosis of injured PACs (Fig. 8A, B, E and F) and improved the viability of PACs induced by TNF-α (Fig. 8C, D, G and H).

3.9. Knockdown of RIPK1 contributed to necrosis of PACs induced by TNF-α in vitro

We further evaluated the possible role of RIPK1 in SAP by RIPK1 siRNA treatment with three individual RIPK1 siRNA sequence. We found that si-RIPK1 (#2) exhibited the highest knockdown efficiency (Fig. 9A and B) and therefore selected this siRNA sequence to knockdown the RIPK1 gene in PACs in our study. Measurement of the necrotic cell percentage using flow cytometry indicated that suppression of RIPK1 promoted the necrosis of PACs (Fig. 9C and D). Meanwhile, the CCK8 assay and LDH release detection both suggested that knockdown of RIPK1 decreased the viability of PACs induced by TNF-α (Fig. 9E and F).

4. Discussion

To date, patients with SAP pose a great challenge to clinicians due to high morbidity and mortality and lack of specific treatment for this disease [22], Neither pancreatic necrosectomy [31], nor antibiotics or probiotics [32] result in satisfactory outcomes. As a consequence of recent findings about the use of MSCs in treating conditions like traumatic injuries of the spinal cord [33], and HBV-related acute liver failure [34], we strongly expect that BMSCs will bring favorable outcomes to patients with SAP. The mechanisms underlying the pathogenesis of SAP are not fully known, but the progression of SAP is frequently accompanied by pancreatic necrosis [35]; hence, reduction of necrosis of injured PACs may be an important therapeutic tactic in the future. Increasing evidence has confirmed that the pathologic process of SAP is associated with the involvement of several miRNAs, of which miR-7, miR-9, miR-122 and miR-141 are noninvasive biomarkers of AP [20]. We investigated the underlying mechanisms by which BMSCs attenuate SAP by upregulating the expression of miR-9 (miR-9-BMSCs) and showed that overexpression of miR-9 in miR-9-BMSCs could significantly promote the therapeutic effects (anti-inflammation and inhibition of necroptosis) to BMSCs alone. Therefore, we believe that miR-9 will play an important therapeutic role for SAP using BMSCs.

SAP is characterized by markedly increased production of many pro-inflammatory mediators, including IL-1β [36], IL-6 [37] and TNF-α [38]. In our study, the levels of serum pro-inflammatory cytokines were much lower in the miR-9-BMSC group than in the BMSC group, as were levels of serum amylase and lipase, and the pathological scores for pancreatic edema, infiltration and acinar necrosis. Our mRNA expression data for pancreatic IL-1β, IL-6 and TNF-α also support this finding. In contrast, anti-inflammatory cytokines IL-4 and IL-10 are believed to be positively correlated with recovery from pancreatic injury [39]. The levels and expression of IL-4 and IL-10 in our study were clearly higher in the miR-9-BMSC group compared with the BMSC group. These results suggest that miR-9-BMSCs exhibit stronger anti-inflammatory effects due to the higher expression of miR-9.

Necroptosis has been confirmed to be a form of programmed cell death that depends on the activation of RIPK1 and RIPK3 by receptors such as TNF receptor-1 [40]. Genetic knockout of RIPK3 was able to alleviate the severity of caerulein-induced AP in mice [41], which demonstrates the role of necroptosis in the development of AP. Therefore, we hold the view that it may be an effective therapeutic treatment to inhibit necroptosis in SAP. Some studies have suggested a relationship between necroptosis and SAP, but the underlying mechanisms still remain unclear. Our studies in vivo and in vitro demonstrated that necroptosis was activated in SAP and expression of RIPK1, RIPK3 and p-MLKL was upregulated after induction by NaT or TNF-α. In addition,

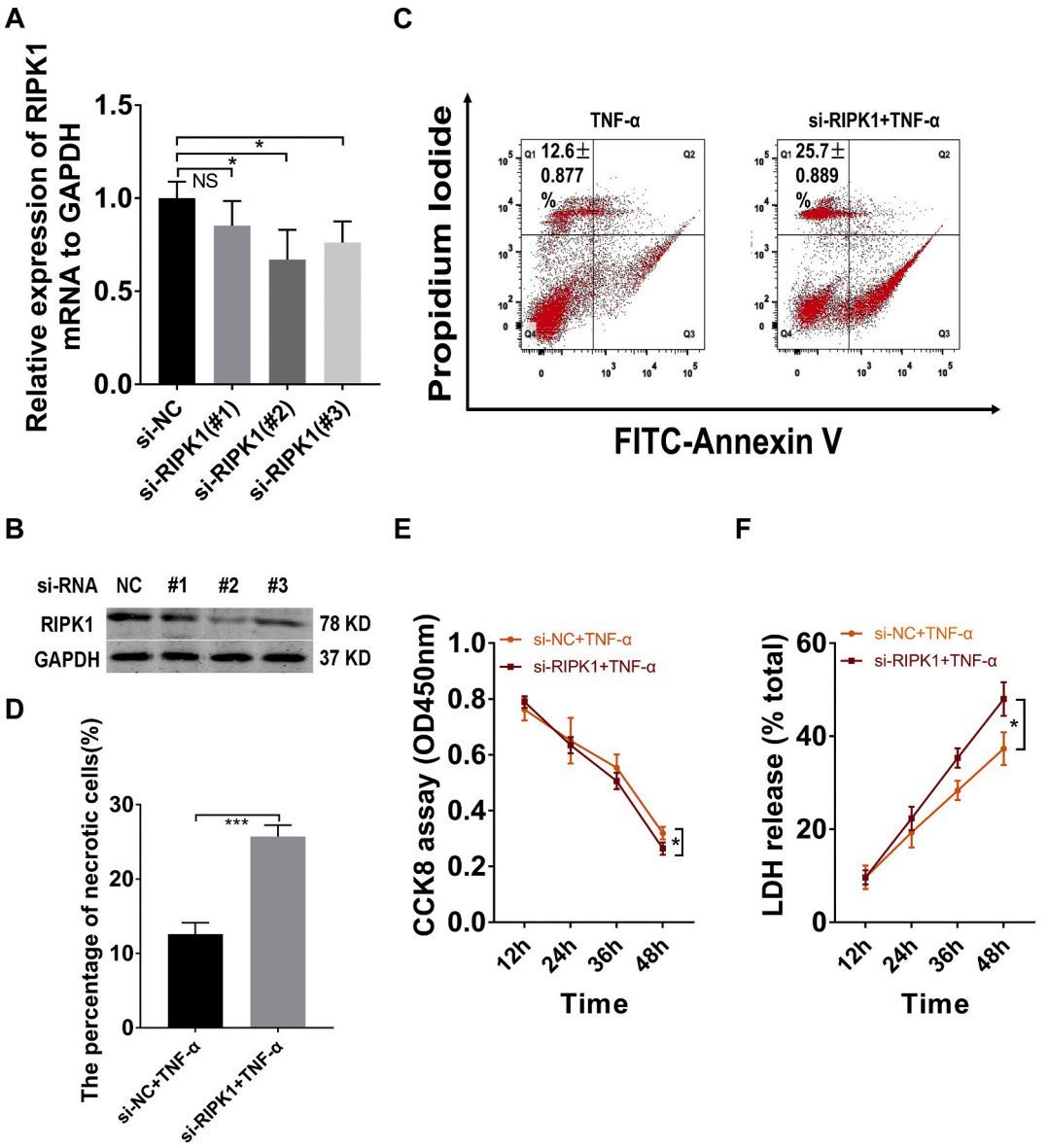

Fig. 9. Knockdown of RIPK1 reduced the viability of PACs treated with TNF-α in vitro.
(A) Relative mRNA expression of RIPK1 in PACs treated with si-NC or si-RIPK1 detected using qRT-PCR. (B) Protein expression of RIPK1 in PACs treated with si-NC or si-RIPK1 measured by western blot. (C) PACs were collected and stained with FITC-Annexin V/PI and analyzed by flow cytometry. Figures are representative of three independent experiments. (D) Analysis of flow cytometric data. (E) CCK-8 assays. (F) LDH release assays. Data are shown as means ± SD from at least three independent experiments. $^{*}p < 0.05$ and $^{***}p < 0.001$; NS, not significant.

miR-9-BMSCs were better able to suppress necroptosis compared with BMSCs. These results indicated that the necroptosis signaling pathway was regulated by miR-9 in BMSC treatment for SAP. We also measured the serum expression of miR-9 from normal donors and AP patients. The level of miR-9 was much higher in SAP compared with MAP patients, showing that miR-9 was associated with the severity of AP. Furthermore, we also examined the expression of miR-9 in pancreatic tissues and found that its expression in the miR-9-BMSC group was markedly higher than in the SAP, PBS or BMSC groups. Hence, miR-9 is likely a crucial factor in the development of SAP, although there are still unknown differences between humans and rats in the mechanism of SAP or AP. We then prepared an miR-9 mimic in the AAV-8 vector and injected it into pancreatic tissues of rats by retrograde pancreaticobiliary injection. We observed that AAV-miR-9 significantly reduced the inflammatory response and enhanced the anti-inflammatory capacity of rats while inhibiting the expression of pancreatic RIPK1 in SAP.

To further investigate the possible molecular mechanism underlying the effect of miR-9 regulating necroptosis, we used miRNA target prediction tools and found that RIPK1 was a potential target of miR-9. We then verified that the RIPK1 gene was the target gene of miR-9 using a dual luciferase reporter system and observed that miR-9 could suppress the expression of RIPK1. In vitro, we found that compared with the BMSC group, miR-9-BMSCs markedly reduced necrosis of PACs induced by TNF-α. In addition, miR-9-BMSCs promoted the survival of PACs. Meanwhile, we transfected the miR-9 mimic into PACs for 24 h followed by incubation with TNF-α for 24 h. Similar to our experiments with miR-9-BMSCs, exogenous miR-9 significantly suppressed necrosis of PACs and enhanced the viability of PACs. It is well known that the RIPK1-RIPK3-MLKL signaling pathway plays an important role in necroptosis but often leads to different outcomes [42]. This includes three different mechanisms as follows: 1) RIPK1-dependent but RIPK3- and MLKL-independent; 2) RIPK3-dependent but RIPK1 and MLKL-independent; and 3) RIPK3 and MLKL-dependent but RIPK1-independent mechanisms [43–45]. To examine which necroptosis pathways were

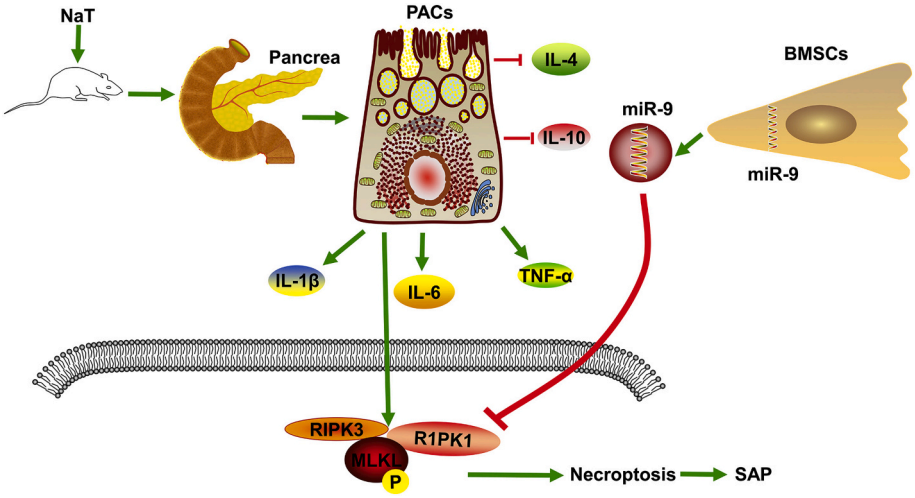

Fig. 10. Schematic of possible mechanisms by which BMSCs inhibit SAP.
After induction of SAP by NaT in rat models, injury of PACs in pancreatic tissues promotes the release of pro-inflammatory cytokines (IL-1β, IL-6 and TNF-α) and reduces the production of anti-inflammatory mediators (IL-4 and IL-10). In addition, the necroptosis pathway is activated, increasing the expression of RIPK1, which binds RIPK3 and p-MLKL as a complex, eventually leading to SAP. miR-9 upregulated by BMSCs targets the RIPK1 gene directly to suppress necroptosis and ultimately ameliorate SAP.

active in SAP, we used siRNA to knockdown RIPK1 and verify the possible role of RIPK1. Interestingly, after si-RIPK1 treatment, there was a significant increase in cell necrosis and significant decrease in the viability of PACs compared with the si-NC group. The results indicated that suppression of RIPK1 by miR-9 or miR-9-BMSCs may inhibit necroptosis, but knockdown of RIPK1 can also promote the death of PACs. These findings at first seemed inconsistent, but we judged the results as accurate after deeper analysis. It has been acknowledged that RIPK1 activity can lead to two disparate consequences: activation of the Nuclear factor κ light chain enhancer of activated B cells (NF-κB) pathway to promote cell viability, or upregulation of necroptosis, resulting in cell death [46]. We hypothesize that the increased necrosis percentage detected in PACs incubated with si-RIPK1 may have resulted from NF-κB-regulated suppression of cell viability. In other words, both excessive overexpression and inactivation of RIPK1 can increase cell necrosis, but normal levels of RIPK1 expression may promote cell survival. A major difference between the inhibition of RIPK1 using miR-9-BMSCs or miR-9 and the knockdown of RIPK1 is that miR-9-BMSCs or miR-9 only suppresses RIPK1-dependent necroptosis but not RIPK1-dependent NF-κB activation, whereas knockdown of RIPK1 impedes both RIPK1-dependent necroptosis and NF-κB activation. The results suggest that RIPK1 could regulate acinar cell survival in SAP.

An increasing number of investigators have focused on pancreatic regeneration in order to alleviate the pains of patients with AP or SAP. In our work, we found that the genes involved in regeneration of pancreas, including PTF1, PDX1, and Reg4, were significantly upregulated after treatment with miR-9-BMSCs. The findings indicated that miR-9 is a key factor involved in pancreatic regeneration of SAP.

In summary, our study strongly suggests that BMSCs can attenuate SAP and promote the regeneration of injured pancreatic tissues by secreting miR-9 to target RIPK1 and inhibit the necroptosis signaling pathway.

5. Conclusions

The present study indicated that administration of miR-9-BMSCs effectively attenuated SAP in vivo and inhibited necroptosis of TNF-α-induced PACs in vitro. miR-9-BMSCs showed anti-inflammatory effects by decreasing cytokines such as IL-1β, IL-6, and TNF-α and increasing anti-inflammatory mediators such as IL-4 and IL-10 and regulating the necroptosis pathway. Besides, miR-9-BMSCs significantly improved the regeneration of injured pancreas. The present results show the potential of miR-9-BMSCs on treating SAP via suppressing necroptosis (Fig. 10).

Conflict of interest

No potential conflicts of interest are disclosed.

Funding statement

The present study was supported by research grants from the National Natural Science Foundation of China (No. 81670582) and College Natural Science Foundation of Anhui Province (KJ2017A271) and talent introduction fund of Yijishan Hospital of Wannan Medical School (YR201601).

Appendix A. Supplementary data

Supplementary data to this article can be found online at https://doi.org/10.1016/j.lfs.2019.03.019.

References

[1] Z.M. Sellers, M. Abu-El-Haija, S.Z. Husain, V. Morinville, New management guidelines for both children and adults with acute pancreatitis, Gastroenterology 155 (2018) 234–235.
[2] P.G. Lankisch, M. Apte, P.A. Banks, Acute pancreatitis, Lancet 386 (2015) 85–96.
[3] B.U. Wu, P.A. Banks, Clinical management of patients with acute pancreatitis, Gastroenterology 144 (2013) 1272–1281.
[4] N.J. Schepers, O.J. Bakker, M.G. Besselink, A.U. Ahmed, T.L. Bollen, H.G. Gooszen, H.C. van Santvoort, M.J. Bruno, Impact of characteristics of organ failure and infected necrosis on mortality in necrotising pancreatitis, Gut (2018) 1–8, https://doi.org/10.1136/gutjnl-2017-314657.
[5] R. Hoque, M. Sohail, A. Malik, S. Sarwar, Y. Luo, A. Shah, F. Barrat, R. Flavell, F. Gorelick, S. Husain, W. Mehal, TLR9 and the NLRP3 inflammasome link acinar cell death with inflammation in acute pancreatitis, Gastroenterology 141 (2011) 358–369.
[6] M. Pasparakis, P. Vandenabeele, Necroptosis and its role in inflammation, Nature 517 (2015) 311–320.
[7] K. Newton, RIPK1 and RIPK3: critical regulators of inflammation and cell death, Trends Cell Biol. 25 (2015) 347–353.
[8] J.E. Morgan, A. Prola, V. Mariot, V. Pini, J. Meng, C. Hourde, J. Dumonceaux, F. Conti, F. Relaix, F.J. Authier, L. Tiret, F. Muntoni, M. Bencze, Publisher correction: necroptosis mediates myofibre death in dystrophin-deficient mice, Nat. Commun. 9 (2018) 4107.
[9] D. Cuchet-Lourenco, D. Eletto, C. Wu, V. Plagnol, O. Papapietro, J. Curtis, L. Ceron-Gutierrez, C.M. Bacon, S. Hackett, B. Alsaleem, M. Maes, M. Gaspar, A. Alisaac, E. Goss, E. AlIdrissi, D. Siegmund, H. Wajant, D. Kumararatne, M.S. AlZahrani, P.D. Arkwright, M. Abinun, R. Doffinger, S. Nejentsev, Biallelic RIPK1 mutations in humans cause severe immunodeficiency, arthritis, and intestinal inflammation,

Science 361 (2018) 810–813.
[10] Y. Xie, S. Zhu, M. Zhong, M. Yang, X. Sun, J. Liu, G. Kroemer, M. Lotze, H.R. Zeh, R. Kang, D. Tang, Inhibition of aurora kinase a induces necroptosis in pancreatic carcinoma, Gastroenterology 153 (2017) 1429–1443.
[11] J. Wu, Z. Huang, J. Ren, Z. Zhang, P. He, Y. Li, J. Ma, W. Chen, Y. Zhang, X. Zhou, Z. Yang, S.Q. Wu, L. Chen, J. Han, Mlkl knockout mice demonstrate the indispensable role of Mlkl in necroptosis, Cell Res. 23 (2013) 994–1006.
[12] M. Hajkova, E. Javorkova, A. Zajicova, P. Trosan, V. Holan, M. Krulova, A local application of mesenchymal stem cells and cyclosporine a attenuates immune response by a switch in macrophage phenotype, J. Tissue Eng. Regen. Med. 11 (2017) 1456–1465.
[13] J.J. Hay, A. Rodrigo-Navarro, M. Petaroudi, A.V. Bryksin, A.J. Garcia, T.H. Barker, M.J. Dalby, M. Salmeron-Sanchez, Bacteria-based materials for stem cell engineering, Adv. Mater. 30 (2018) e1804310.
[14] A.P. Johnston, S.A. Yuzwa, M.J. Carr, N. Mahmud, M.A. Storer, M.P. Krause, K. Jones, S. Paul, D.R. Kaplan, F.D. Miller, Dedifferentiated Schwann cell precursors secreting paracrine factors are required for regeneration of the mammalian digit tip, Cell Stem Cell 19 (2016) 433–448.
[15] J. Gong, H.B. Meng, J. Hua, Z.S. Song, Z.G. He, B. Zhou, M.P. Qian, The SDF-1/CXCR4 axis regulates migration of transplanted bone marrow mesenchymal stem cells towards the pancreas in rats with acute pancreatitis, Mol. Med. Rep. 9 (2014) 1575–1582.
[16] D. Qian, J. Gong, Z. He, J. Hua, S. Lin, C. Xu, H. Meng, Z. Song, Bone marrow-derived mesenchymal stem cells repair necrotic pancreatic tissue and promote angiogenesis by secreting cellular growth factors involved in the SDF-1 alpha /CXCR4 axis in rats, Stem Cells Int. 2015 (2015) 306836.
[17] Z. He, J. Hua, D. Qian, J. Gong, S. Lin, C. Xu, G. Wei, H. Meng, T. Yang, B. Zhou, Z. Song, Intravenous hMSCs ameliorate acute pancreatitis in mice via secretion of tumor necrosis factor-alpha stimulated gene/protein 6, Sci. Rep. 6 (2016) 38438.
[18] D. Qian, G. Wei, C. Xu, Z. He, J. Hua, J. Li, Q. Hu, S. Lin, J. Gong, H. Meng, B. Zhou, H. Teng, Z. Song, Bone marrow-derived mesenchymal stem cells (BMSCs) repair acute necrotized pancreatitis by secreting microRNA-9 to target the NF-kappaB1/p50 gene in rats, Sci. Rep. 7 (2017) 581.
[19] T. Treiber, N. Treiber, G. Meister, Author correction: regulation of microRNA biogenesis and its crosstalk with other cellular pathways, Nat. Rev. Mol. Cell Biol. 19 (2018) 808.
[20] P. Lu, F. Wang, J. Wu, C. Wang, J. Yan, Z.L. Li, J.X. Song, J.J. Wang, Elevated serum miR-7, miR-9, miR-122, and miR-141 are noninvasive biomarkers of acute pancreatitis, Dis. Markers 2017 (2017) 7293459.
[21] C.X. Li, N.P. Talele, S. Boo, A. Koehler, E. Knee-Walden, J.L. Balestrini, P. Speight, A. Kapus, B. Hinz, MicroRNA-21 preserves the fibrotic mechanical memory of mesenchymal stem cells, Nat. Mater. 16 (2017) 379–389.
[22] O.J. Bakker, S. van Brunschot, H.C. van Santvoort, M.G. Besselink, T.L. Bollen, M.A. Boermeester, C.H. Dejong, H. van Goor, K. Bosscha, A.U. Ahmed, S. Bouwense, W.M. van Grevenstein, J. Heisterkamp, A.P. Houdijk, J.M. Jansen, T.M. Karsten, E.R. Manusama, V.B. Nieuwenhuijs, A.F. Schaapherder, G.P. van der Schelling, M.P. Schwartz, B.W. Spanier, A. Tan, J. Vecht, B.L. Weusten, B.J. Witteman, L.M. Akkermans, M.J. Bruno, M.G. Dijkgraaf, B. van Ramshorst, H.G. Gooszen, Early versus on-demand nasoenteric tube feeding in acute pancreatitis, N. Engl. J. Med. 371 (2014) 1983–1993.
[23] S.G. Willet, M.A. Lewis, Z.F. Miao, D. Liu, M.D. Radyk, R.L. Cunningham, J. Burclaff, G. Sibbel, H.G. Lo, V. Blanc, N.O. Davidson, Z.N. Wang, J.C. Mills, Regenerative proliferation of differentiated cells by mTORC1-dependent paligenosis, EMBO J. (2018) 37.
[24] D. Grimm, K. Pandey, H. Nakai, T.A. Storm, M.A. Kay, Liver transduction with recombinant adeno-associated virus is primarily restricted by capsid serotype not vector genotype, J. Virol. 80 (2006) 426–439.
[25] G. Hu, J. Shen, L. Cheng, C. Guo, X. Xu, F. Wang, L. Huang, L. Yang, M. He, D. Xiang, S. Zhu, M. Wu, Y. Yu, W. Han, X. Wang, Reg4 protects against acinar cell necrosis in experimental pancreatitis, Gut 60 (2011) 820–828.
[26] J.H. Kim, H.W. Kim, K.J. Cha, J. Han, Y.J. Jang, D.S. Kim, J.H. Kim, Nanotopography promotes pancreatic differentiation of human embryonic stem cells and induced pluripotent stem cells, ACS Nano 10 (2016) 3342–3355.
[27] D. Hesselson, R.M. Anderson, D.Y. Stainier, Suppression of Ptf1a activity induces acinar-to-endocrine conversion, Curr. Biol. 21 (2011) 712–717.
[28] L.M. Friedman, A.A. Dror, E. Mor, T. Tenne, G. Toren, T. Satoh, D.J. Biesemeier, N. Shomron, D.M. Fekete, E. Hornstein, K.B. Avraham, MicroRNAs are essential for development and function of inner ear hair cells in vertebrates, Proc. Natl. Acad. Sci. U. S. A. 106 (2009) 7915–7920.
[29] H. Dweep, C. Sticht, P. Pandey, N. Gretz, MiRWalk-database: prediction of possible miRNA binding sites by "walking" the genes of three genomes, J. Biomed. Inform. 44 (2011) 839–847.
[30] D. Betel, M. Wilson, A. Gabow, D.S. Marks, C. Sander, The microRNA.org resource: targets and expression, Nucleic Acids Res. 36 (2008) D149–D153.
[31] H. Seifert, M. Biermer, W. Schmitt, C. Jurgensen, U. Will, R. Gerlach, C. Kreitmair, A. Meining, T. Wehrmann, T. Rosch, Transluminal endoscopic necrosectomy after acute pancreatitis: a multicentre study with long-term follow-up (the GEPARD study), GUT 58 (2009) 1260–1266.
[32] G.P. Bongaerts, R.S. Severijnen, A reassessment of the PROPATRIA study and its implications for probiotic therapy, Nat. Biotechnol. 34 (2016) 55–63.
[33] H.Y. Kim, H. Kumar, M.J. Jo, J. Kim, J.K. Yoon, J.R. Lee, M. Kang, Y.W. Choo, S.Y. Song, S.P. Kwon, T. Hyeon, I.B. Han, B.S. Kim, Therapeutic efficacy-potentiated and diseased organ-targeting nanovesicles derived from mesenchymal stem cells for spinal cord injury treatment, Nano Lett. 18 (2018) 4965–4975.
[34] B.L. Lin, J.F. Chen, W.H. Qiu, K.W. Wang, D.Y. Xie, X.Y. Chen, Q.L. Liu, L. Peng, J.G. Li, Y.Y. Mei, W.Z. Weng, Y.W. Peng, H.J. Cao, J.Q. Xie, S.B. Xie, A.P. Xiang, Z.L. Gao, Allogeneic bone marrow-derived mesenchymal stromal cells for hepatitis B virus-related acute-on-chronic liver failure: a randomized controlled trial, Hepatology 66 (2017) 209–219.
[35] G.I. Papachristou, V. Muddana, D. Yadav, M. O'Connell, M.K. Sanders, A. Slivka, D.C. Whitcomb, Comparison of BISAP, Ranson's, APACHE-II, and CTSI scores in predicting organ failure, complications, and mortality in acute pancreatitis, Am. J. Gastroenterol. 105 (435-441) (2010) 442.
[36] P. Noel, K. Patel, C. Durgampudi, R.N. Trivedi, C. de Oliveira, M.D. Crowell, R. Pannala, K. Lee, R. Brand, J. Chennat, A. Slivka, G.I. Papachristou, A. Khalid, D.C. Whitcomb, J.P. DeLany, R.A. Cline, C. Acharya, D. Jaligama, F.M. Murad, D. Yadav, S. Navina, V.P. Singh, Peripancreatic fat necrosis worsens acute pancreatitis independent of pancreatic necrosis via unsaturated fatty acids increased in human pancreatic necrosis collections, Gut 65 (2016) 100–111.
[37] M. Merza, H. Hartman, M. Rahman, R. Hwaiz, E. Zhang, E. Renstrom, L. Luo, M. Morgelin, S. Regner, H. Thorlacius, Neutrophil extracellular traps induce trypsin activation, inflammation, and tissue damage in mice with severe acute pancreatitis, Gastroenterology 149 (2015) 1920–1931.
[38] M. Sendler, A. Dummer, F.U. Weiss, B. Kruger, T. Wartmann, K. Scharffetter-Kochanek, N. van Rooijen, S.R. Malla, A. Aghdassi, W. Halangk, M.M. Lerch, J. Mayerle, Tumour necrosis factor alpha secretion induces protease activation and acinar cell necrosis in acute experimental pancreatitis in mice, Gut 62 (2013) 430–439.
[39] K. Robinson, L. Vona-Davis, D. Riggs, B. Jackson, D. McFadden, Peptide YY attenuates STAT1 and STAT3 activation induced by TNF-alpha in acinar cell line AR42J, J. Am. Coll. Surg. 202 (2006) 788–796.
[40] M. Mompean, W. Li, J. Li, S. Laage, A.B. Siemer, G. Bozkurt, H. Wu, A.E. McDermott, The structure of the necrosome RIPK1-RIPK3 core, a human hetero-amyloid signaling complex, Cell 173 (2018) 1244–1253.
[41] N. Yatim, H. Jusforgues-Saklani, S. Orozco, O. Schulz, D.S.R. Barreira, E.S.C. Reis, D.R. Green, A. Oberst, M.L. Albert, RIPK1 and NF-kappaB signaling in dying cells determines cross-priming of CD8(+) T cells, Science 350 (2015) 328–334.
[42] L.A. Barbosa, P.P. Fiuza, L.J. Borges, F.A. Rolim, M.B. Andrade, N.F. Luz, G. Quintela-Carvalho, J.B. Lima, R.P. Almeida, F.K. Chan, M.T. Bozza, V.M. Borges, D.B. Prates, RIPK1-RIPK3-MLKL-associated necroptosis drives Leishmania infantum killing in neutrophils, Front. Immunol. 9 (2018) 1818.
[43] W.J. Kaiser, H. Sridharan, C. Huang, P. Mandal, J.W. Upton, P.J. Gough, C.A. Sehon, R.W. Marquis, J. Bertin, E.S. Mocarski, Toll-like receptor 3-mediated necrosis via TRIF, RIP3, and MLKL, J. Biol. Chem. 288 (2013) 31268–31279.
[44] D.K. Vo, Y. Urano, W. Takabe, Y. Saito, N. Noguchi, 24(S)-hydroxycholesterol induces RIPK1-dependent but MLKL-independent cell death in the absence of caspase-8, Steroids 99 (2015) 230–237.
[45] S. Saveljeva, L.S. Mc, P. Vandenabeele, A. Samali, M.J. Bertrand, Endoplasmic reticulum stress induces ligand-independent TNFR1-mediated necroptosis in L929 cells, Cell Death Dis. 6 (2015) e1587.
[46] D.E. Christofferson, J. Yuan, Necroptosis as an alternative form of programmed cell death, Curr. Opin. Cell Biol. 22 (2010) 263–268.